

Copyright © 1992, by the author(s).
All rights reserved.

Permission to make digital or hard copies of all or part of this work for personal or classroom use is granted without fee provided that copies are not made or distributed for profit or commercial advantage and that copies bear this notice and the full citation on the first page. To copy otherwise, to republish, to post on servers or to redistribute to lists, requires prior specific permission.

**SIGNAL AMPLIFICATION VIA CHAOS:
EXPERIMENTAL EVIDENCE**

by

K. S. Halle, L. O. Chua, V. S. Anishchenko,
and M. A. Safonova

Memorandum No. UCB/ERL M92/130

25 November 1992

UCB/ERL M92/130

**SIGNAL AMPLIFICATION VIA CHAOS:
EXPERIMENTAL EVIDENCE**

by

K. S. Halle, L. O. Chua, V. S. Anishchenko,
and M. A. Safonova

Memorandum No. UCB/ERL M92/130

25 November 1992

ELECTRONICS RESEARCH LABORATORY

College of Engineering
University of California, Berkeley
94720

TITLE PAGE

**SIGNAL AMPLIFICATION VIA CHAOS:
EXPERIMENTAL EVIDENCE**

by

K. S. Halle, L. O. Chua, V. S. Anishchenko,
and M. A. Safonova

Memorandum No. UCB/ERL M92/130

25 November 1992

ELECTRONICS RESEARCH LABORATORY

College of Engineering
University of California, Berkeley
94720

SIGNAL AMPLIFICATION VIA CHAOS: EXPERIMENTAL EVIDENCE

K. S. Halle, L. O. Chua
*Electronics Research Laboratory,
 Department of Electrical Engineering and Computer Sciences,
 University of California, Berkeley, CA 94720, U. S. A.*

V. S. Anishchenko, M. A. Safonova
Physics Department, Saratov State University, Saratov, Russia

Abstract

Experimental evidence showing the existence of signal amplification via perturbation of periodic and chaotic orbits in an electronic circuit is presented.

1 Introduction

Chua's circuit [Chua, 1992] shown in Fig. 1a, is a simple oscillator circuit which exhibits a variety of bifurcation and chaotic phenomena. The circuit contains three linear energy-storage elements (an inductor and two capacitors), a linear resistor, and a single nonlinear resistor, called Chua's diode [Kennedy, 1992a; Kennedy, 1992b]. The Chua's diode has a five-segment piecewise-linear driving point characteristic, as shown in Fig. 1b, and has been implemented as an integrated circuit [Cruz & Chua, 1992]. It has proven invaluable in many studies of chaotic behavior because it is the simplest and most robust electronic circuit for generating chaotic signals.

The state equations which describe Chua's circuit are given by:

$$\begin{aligned}\frac{dv_{C_1}}{dt} &= \frac{1}{C_1} \left(\frac{v_{C_2} - v_{C_1}}{R} - \hat{f}(v_{C_1}) \right) \\ \frac{dv_{C_2}}{dt} &= \frac{1}{C_2} \left(\frac{v_{C_1} - v_{C_2}}{R} + i_L \right) \\ \frac{di_L}{dt} &= \frac{1}{L} (-v_{C_2})\end{aligned}\tag{1}$$

where

$$i_R = \hat{f}(v_R) = G_b v_R + \frac{1}{2}(G_a - G_b) [|v_R + B_p| - |v_R - B_p|] + \frac{1}{2}(\hat{G} - G_a) [|v_R + \hat{B}_p| + |v_R - \hat{B}_p| - 2\hat{B}_p]$$

These equations can be transformed into the following dimensionless form by a change of variables:

$$\begin{aligned}\dot{x} &= \alpha(y - x - f(x)) \\ \dot{y} &= x - y + z \\ \dot{z} &= -\beta y\end{aligned}\tag{2}$$

where

$$f(x) = m_1 x + \frac{1}{2}(m_0 - m_1)[|x + 1| - |x - 1|] + \frac{1}{2}(\hat{m} - m_0)[|x + k| + |x - k| - 2k]$$

Here, m_1 , m_0 , α and β , \hat{m} and k are the control parameters of the system.¹ The most commonly and easily varied parameters are α and β . In the experiments we will vary the parameter α which is equal to C_2/C_1 , while leaving β fixed at 14.28.

An experimentally derived diagram showing the five possible types of dynamic behavior as a function of α and β is given in Fig. 2. The five regions represent the parameter regions in which the following attractors emerge, from left to right: fixed point (FP), limit cycle (LC), Rössler-type (R), Double Scroll (DS), and outer limit cycle (OLC). Typical spectra for each type of attractor are given in Fig. 3a through Fig. 3e. The state variable used to generate the spectrum is v_{C_1} (which corresponds to x in the dimensionless form).

2 Discussion of Experimental Results

In this section we show the experimental results obtained. The first system setup we used is shown in Fig. 4a. Here, the input sinusoidal signal is injected as a voltage in series with the inductor. We consider the voltage across capacitor C_1 as the output signal. The circuit parameters we use are $C_2 = 99.8nF$, $R = 1604\Omega$, $L = 19.36mH$, $G_a = -0.445mS$, $G_b = -0.713mS$, $B_p = 1.0V$, $\hat{B}_p = 7.2V$ and $\hat{G} = 4.6mS$. We will vary α by varying C_1 . Figure 5b shows the input and output spectra for a particular input signal. The system is operating in the Rössler region. Note the small ‘‘horns’’ which appear at the input frequency, and at the frequencies which are equal to the difference and sum between the Rössler center frequency and the input frequency. It is the presence of these discernible ‘‘horns’’, or peaks, which leads us to conclude that the input signal is being amplified. Fig 5a shows the Rössler spectrum before the input is applied for comparison. The voltage gain in this case is approximately 50dB.

2.1 Gain vs the parameter α

As we vary the parameter α (corresponding to varying C_1 in the circuit) from the FP region to the OLC region, and measure the voltage gain at a fixed input signal amplitude and frequency, we obtain the graph shown in Fig. 6. Here we see that the gain changes as the dynamics of the circuit change.

In the FP region, the gain observed is exactly the same as that calculated by removing all dynamic elements. That is, if the inductor is shorted, and all capacitors removed, we are left with a positive linear resistance in series with a resistor having a negative non-linear resistance. This non-linear voltage divider gives a gain of 12dB.

We then see a sharp rise in gain as the dynamics of the circuit come into play in the limit cycle region. We also see the rise of a multiplicative effect. Figure 7 shows the input and output

¹The parameters \hat{m} and k belong to the outermost segments in the Chua’s diode and play a role only in the dynamics of the outer limit cycle.

spectra when the system is in the limit cycle region. The large peak in the center is the limit cycle frequency. Surrounding that are peaks at the sums and differences of the input and limit cycle frequencies. These sum and difference frequencies are the results of time-domain multiplication of the input signal and the limit cycle frequency. This behavior is similar to that which occurs in parametric amplifiers [Chua, 1969; Brandt, 1982].

Fig. 8 shows a different view of behavior in the limit cycle region. When the input frequency is close to a subharmonic of the limit cycle frequency, and of sufficient strength, peaks will occur at multiples of the difference between the input signal, and the subharmonic. Further, these peaks are at multiples of the periodicity of the limit cycle containing the subharmonic. Thus, when the input is near $1/3$ of the limit cycle frequency, peaks appear at the input frequency plus and minus integer multiples of three times the distance between the input frequency and $1/3$ the limit cycle frequency. Fig 9. shows a computer simulation verifying this behavior.

In this and later computer simulations, we have added a resistance of 36.6Ω in series with the inductor to account for the series resistance of the inductor. The discrepancies in the component values between the computer simulations and the experimental setup are due to parasitic components which we did not include in the model.

At the transition from LC to Rössler, we see another sharp jump in gain as the circuit dynamics change. Although not evident at this particular choice of signal frequency and amplitude, the Rössler region has the highest overall measured gain.

In the Double Scroll region, the gain continues to increase. Note that there are dips in gain as α is varied. On either side of each dip is a peak. We observe from the experiments that each dip corresponds to a periodic window in the Double Scroll region. As the window is approached from either side by varying the parameters, the gain increases as the general level of chaotic energy increases. Then, in the window, the chaotic energy sharply decreases, as does the gain.

Finally, in the outer limit cycle region, the gain drops sharply. Gain is still present for some choices of α , but is generally low.

2.2 Gain vs Frequency of input signal

Holding the input amplitude fixed and α fixed in the Rössler region, and varying the input frequency, we obtain the graph shown in Fig. 10. For comparison, the spectrum of the Rössler attractor at this parameter setting with no input signal applied is given in Fig. 11. Note that the general shape of the two curves is very similar.

At the Rössler center frequency, the input has no effect on the system. Thus the graph has a sharp dip at this frequency.

The region of the two "humps" in the unperturbed spectrum of the attractor proves to provide the highest gain. The particular choice of parameters is close to a periodic window in the Rössler region. Each of these humps is located near where a peak will occur when the periodic window is entered. This fact will be referred to later as well.

A computer simulation has generated the equivalent graph of gain versus input frequency as shown in Fig. 12. The algorithm used to generate this graph subtracts the unperturbed spectrum from the perturbed spectrum in order to eliminate apparent gain at frequencies at which the signal is not detectable above the chaotic energy for the number of points used in our DFT. Because the shape of the spectrum changes with the input applied, this algorithm gives a few dips in gain where none should exist. The computer generated spectrum of the unperturbed attractor is also given in Fig. 13 for comparison.

2.3 Gain vs Amplitude of input signal

The plot of gain as a function of input signal amplitude at a fixed frequency of 1kHz in the Rössler region is shown in Fig. 14. The curve is roughly linear, implying an inverse relationship between input amplitude and gain. Three dips can be seen in the curve. Each of these takes place at the transition between attractors. At -51.5dBV, the input sinusoid kicks the system onto the Double Scroll attractor. There is a periodic window when the system is excited at -20dBv. The system is kicked onto the outer limit cycle at -12.5dBV, and onto an intermittent mixture of the outer limit cycle and the Double Scroll at -4.4dBV.

2.4 Conjectures

We conjecture the existence of four distinct mechanisms which are responsible for the observed voltage gain in different regions. The first is the gain observed in the system without dynamics. This is well predicted by non-linear circuit theory [Chua, 1969]. The second is a general mechanism which we conjecture will be present in any attractor. This is currently being studied. The third we feel is a form of resonance. The fourth gain mechanism occurs only when the system exhibits the Double Scroll attractor. We conjecture this mechanism is due to the input signal modifying the behavior of switching between the Rössler attractors which are inside the Double Scroll.

To clarify the third mechanism, that of a form of resonance, refer back to the gain vs frequency plot of Fig. 10. The parameter α at which this Rössler attractor occurs was specifically chosen to be near a period three window. Fig. 15 shows the spectrum of a periodic orbit in this periodic window. The humps in the Rössler attractor are observed to move toward, and become the peaks seen in the periodic window as α is varied. Further, the peak in gain is seen to narrow in bandwidth while increase in amplitude as α is varied in the direction of this periodic window. The peak in gain seen near these humps is thus a type of resonance between the input signal and this period-three orbit. There also exists a stable period-five window. The same behavior is seen to exist near this periodic window as well.

The fourth mechanism has been discussed in [Anishchenko et al, 1992]. The behavior seen here is similar to the simulation results in [Anishchenko et al, 1992]. Fig 16 shows the probability of the system to reside in one Rössler attractor for the duration τ , with an input signal applied. As discussed in [Anishchenko et al, 1992], this curve has the characteristic shape associated with the classical stochastic resonance (SR) phenomenon. However, no gain is observed in classical SR systems. The gain observed in our case is due to the chaotic dynamics providing energy which is then modified by the input signal.

2.5 Implications

The Rössler region is especially amenable to synchronization. Experiments carried out in [Kocarev et al., 1992] have shown that reductions in the chaotic deterministic noise of 40dB or more are possible. Initial trials have indicated that synchronization still takes place with the signal injected. Future experiments are planned to determine if this can be exploited to give amplification with high Signal-to-Noise-Ratio (SNR) at the output. Due to the non-linear gain, it might also be possible to obtain amplification while actually improving the signal to noise ratio, for a range of input signal to noise ratios, frequencies, and intensities.

2.6 Signal Injection Points

We have considered various placements of the driving signal at fixed α , β , input signal amplitude, and frequency. See Fig. 4b, 4c, 4d. Figure 17a shows input and output when the inductor is driven, for comparison with the other driving points. Figure 17b shows that driving capacitor C_2 significantly reduces the gain, as does driving capacitor C_1 , shown in Fig. 17b. However, the voltage source in series with the nonlinear resistor gives nearly indistinguishable behavior from one in series with the inductor, and shown in (Fig. 17d). In addition, these may be more appropriate drive points when considering synchronization of chaotic circuits.

Fig. 18 shows that considering the voltage across capacitor C_2 as the output voltage also gives less gain.

3 Conclusion

We have seen voltage gains as high as 56dB from a non-linear circuit operating in the chaotic regime. In the limit cycle region and the Rössler region, the behavior is similar to that which arises in parametric amplifiers. In the Rössler region, we have a form of resonance increasing the gain. In the Double Scroll region, modification of switching behavior similar to stochastic resonance was conjectured to be responsible for the gain. This is the first time such general gain phenomena have been reported.

These results have exciting potential for low-noise amplification and high-sensitivity detector applications.

4 Acknowledgements

This work was sponsored in part by the National Science Foundation under Grant MIP 89-12639 and by the Office of Naval Research under Grant N00014-89-J-1402. Special thanks to Bert Shi for many interesting conversations on the contents of this paper, and for further ideas to pursue.

References

- Chua, L. O. [1992] "The genesis of Chua's circuit," *Archiv für Elektronik und Übertragungstechnik*, 46(4), 250-257.
- Cruz, J. M. & Chua, L. O. [1992] "A CMOS IC nonlinear resistor for Chua's circuit," *IEEE Trans. on Circuits and Systems*, 39(11), in press.
- Kennedy, M. P. [1992a] "Experimental chaos via Chua's circuit", *Proceedings of the 1st Experimental Chaos Conference, Arlington, Virginia*, edited by S. Vohra et al., World Scientific, 340-351.
- Kennedy, M. P. [1992b] "Robust OP Amp realization of Chua's circuit," *Frequenz*, 46(3-4), 66-80.
- Chua, L. O. [1969] "Introduction to nonlinear network theory", McGraw-Hill, New York.
- Brandt, L. [1982] "Parametric Electronics," *Springer Series in Electrophysics 6*, Springer-Verlag.

- Anishchenko, V. S., Safonova, M. A., & Chua, L. O. [1992]** "Stochastic resonance in Chua's circuit", *Int. Journal of Bifurcation and Chaos*, 2(2), 397-401.
- Kocarev, Lj., Halle, K. S., Eckert, K., Parlitz, U. & Chua, L. O. [1992]** "Experimental demonstration of secure communication via chaotic synchronization", *Int. J. Bifurcation and Chaos*, 2(3), in press.

Figure Captions

Figure 1a: Chua's Circuit.

Figure 1b: Piecewise-linear characteristic of nonlinear resistor.

Figure 2: Experimentally derived $\alpha - \beta$ diagram showing regions of different dynamic behavior.

Figure 3: Spectrum of different types of attractors.

- (a) fixed point, $\alpha = 4.88$, BW of spectrum = 10kHz.
- (b) limit cycle, $\alpha = 9.56$, BW of spectrum = 10kHz.
- (c) Rössler-type attractor, $\alpha = 10.26$, BW of spectrum = 10kHz.
- (d) Double Scroll attractor, $\alpha = 10.70$, BW of spectrum = 10kHz.
- (e) outer limit cycle, $\alpha = 12.98$, BW of spectrum = 25kHz.

Figure 4: Different injection points. The input signal is applied at

- (a) the inductor L .
- (b) the capacitor C_2 .
- (c) the capacitor C_1 .
- (d) the Chua's diode N_R .

Figure 5: Spectra in the Rössler region. $\alpha = 10.26$, $F_{in} = 850\text{Hz}$ at -70dBV . BW of spectrum = 2.5kHz

- (a) With no input applied.
- (b) With input applied.

Figure 6: Gain versus the parameter α . $F_{in} = 1\text{kHz}$ @ -70dBV .

Figure 7: Input and output spectra in the limit cycle region. $\alpha = 9.75$, $F_{in} = 840\text{Hz}$ @ -70.0dBV .

Figure 8: Output spectra in the limit cycle region. $\alpha = 9.75$, $F_{in} = 902\text{Hz}$ @ -50.0dBV .

Figure 9: Computer simulation of the output spectra before and after an input is applied. $\alpha = 9.35$, $F_{in} = 902\text{Hz}$ @ -50.0dBV .

Figure 10: Gain versus frequency of the input signal. $\alpha = 10.12$, F_{in} @ -70.0dBV .

Figure 11: Spectrum of the Rössler attractor used for Fig 10. $\alpha = 10.12$, no input.

Figure 12: Gain versus frequency of the input signal from a computer simulation. $\alpha = 9.80$, F_{in} @ -70.0dBV .

Figure 13: Spectrum of the Rössler attractor used in Fig 12. $\alpha = 9.80$, no input

Figure 14: Gain versus amplitude of input signal. $F_{in} = 1\text{kHz}$.

Figure 15: Spectrum of a periodic orbit in the period 3 window. $\alpha = 10.16$, no input.

Figure 16: Probability of the system to reside in one Rössler attractor for the duration τ . $\alpha = 11.04$, $F_{in} = 371\text{Hz}$ @ -56dBV , $\tau = t/T$ where $T = 1/F_{in}$, t in sec.

Figure 17: Spectra of input and output when

- (a) inductor driven, for comparison.
- (b) capacitor C_2 is driven.
- (c) capacitor C_1 is driven.
- (d) superposition of outputs when drive is in series with inductor and nonlinear resistor. $\alpha = 10.51$ (DS attractor), $F_{in} = 500\text{Hz}$ @ -51dBV .

Figure 18: Spectra comparing outputs at V_{C_1} and V_{C_2} .

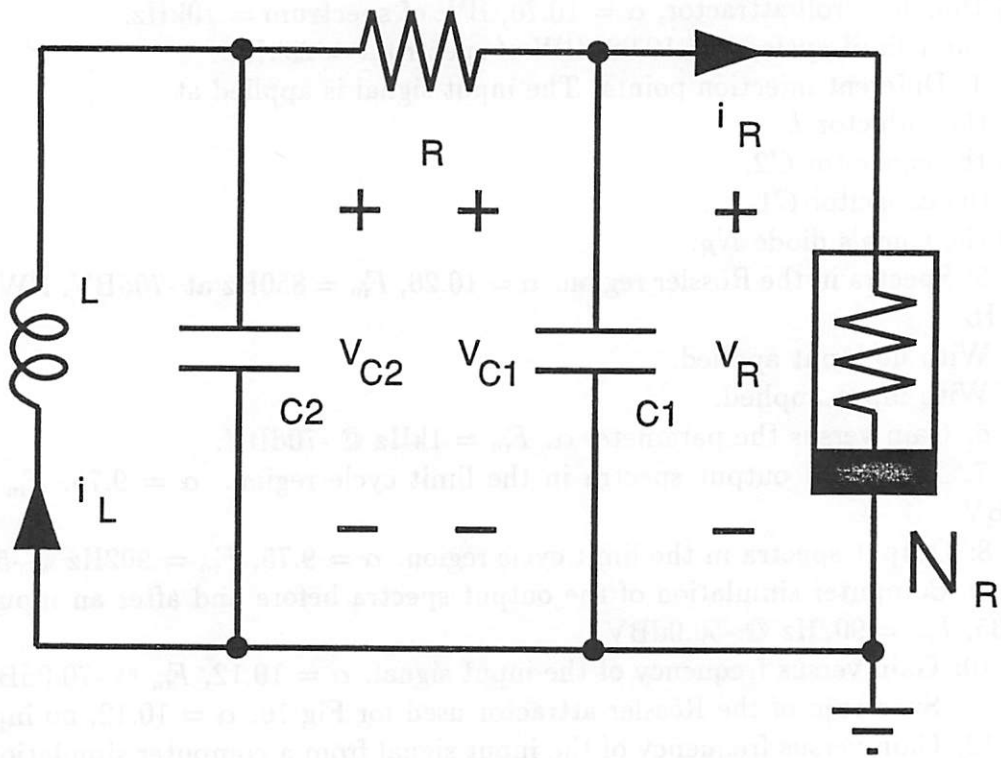


FIGURE 1a

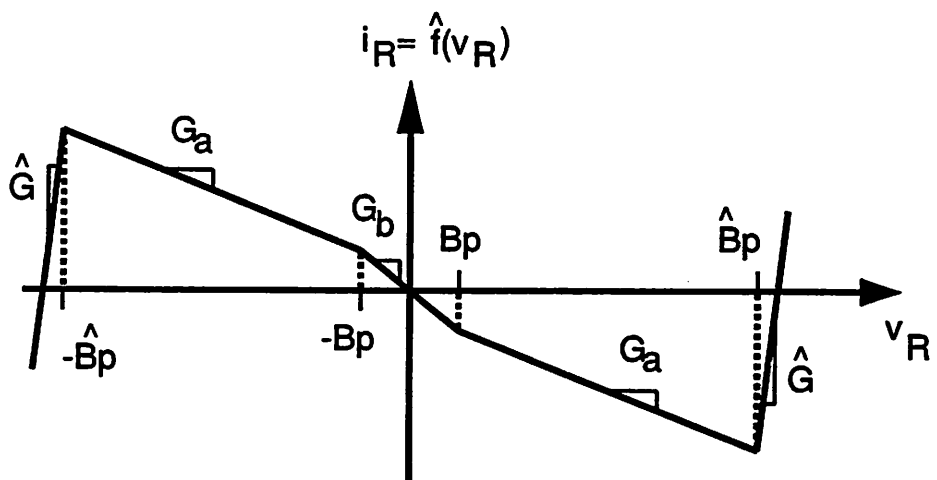


Figure 1 b

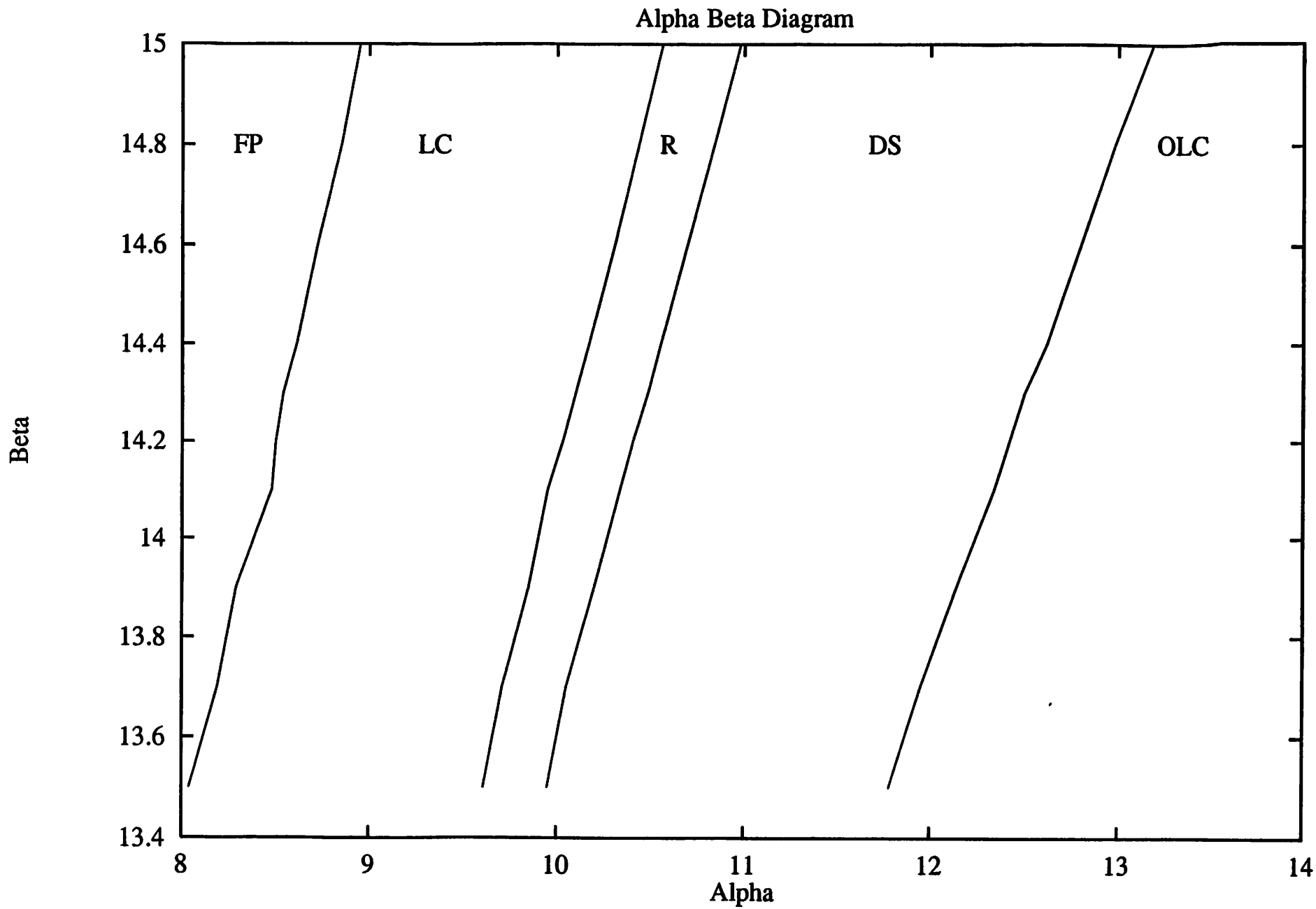


FIGURE 2

fig3a.tif

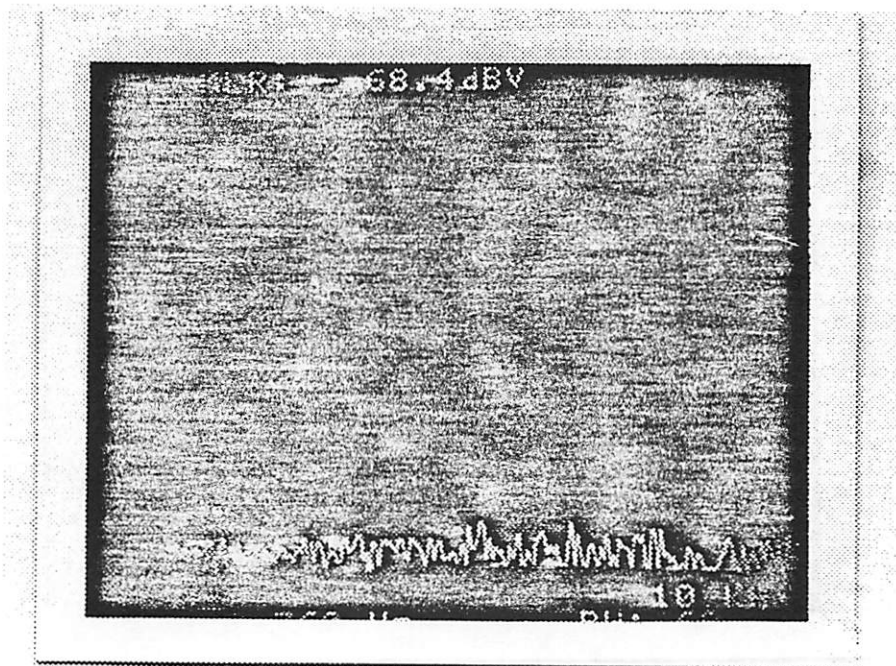


Figure 3a

fig3b.tif

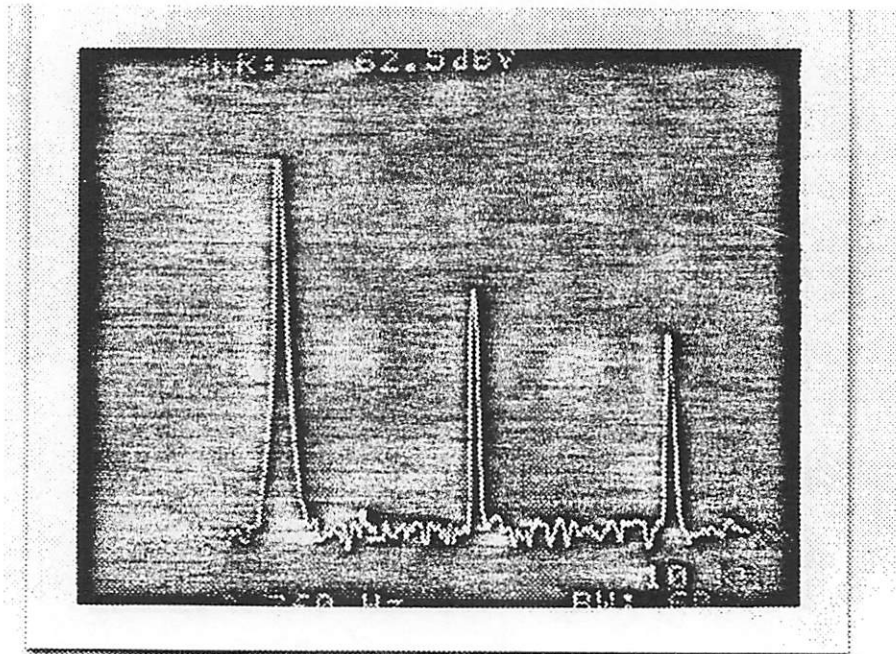


Figure 3b

fig3c.tif

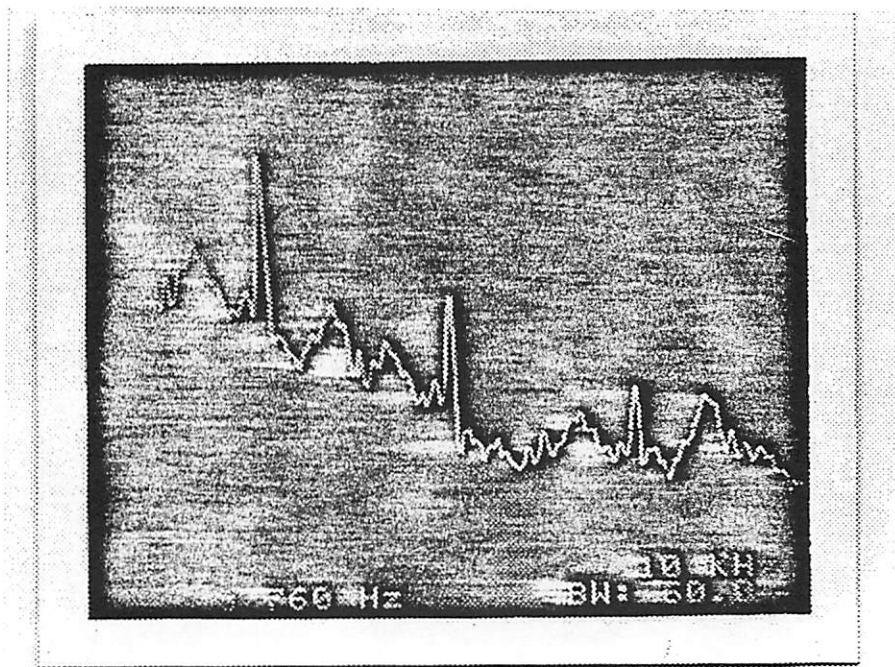


Figure 3c

fig3d.tif

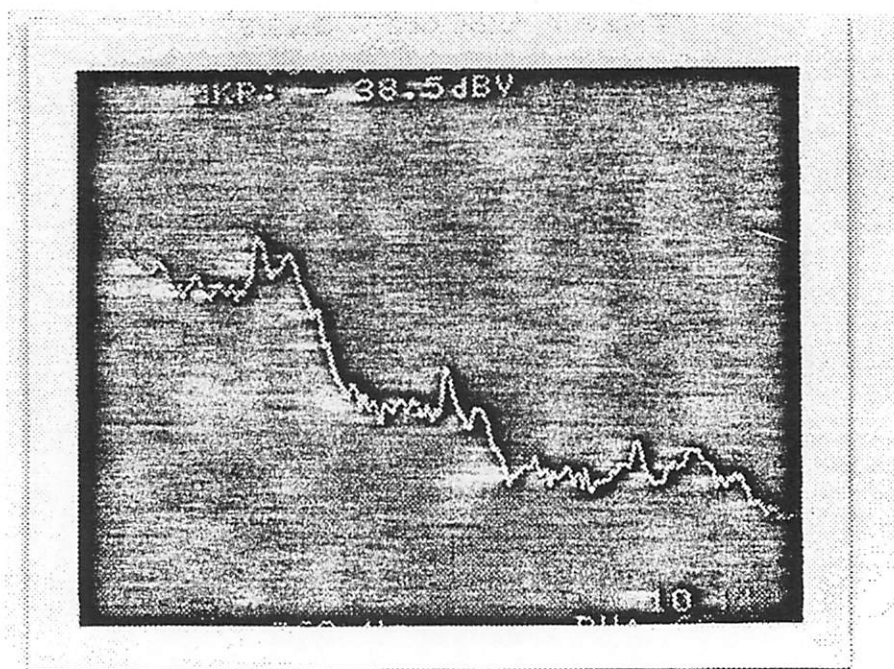


Figure 3d

fig3e.tif

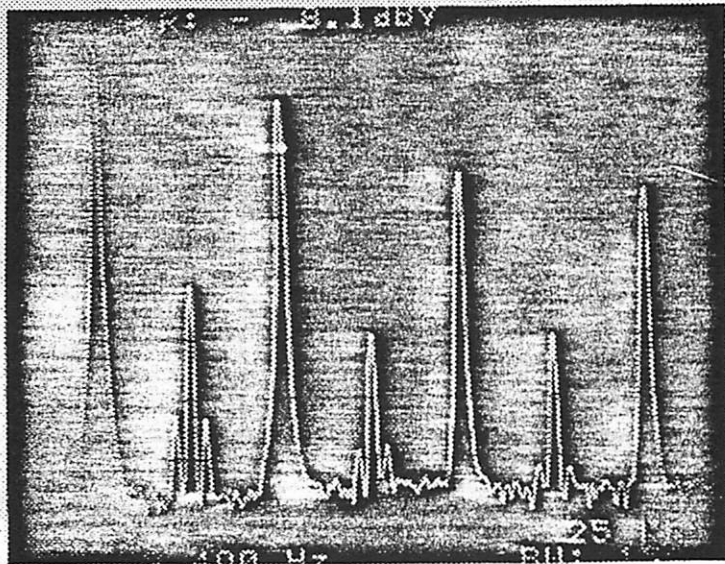


Figure 3e

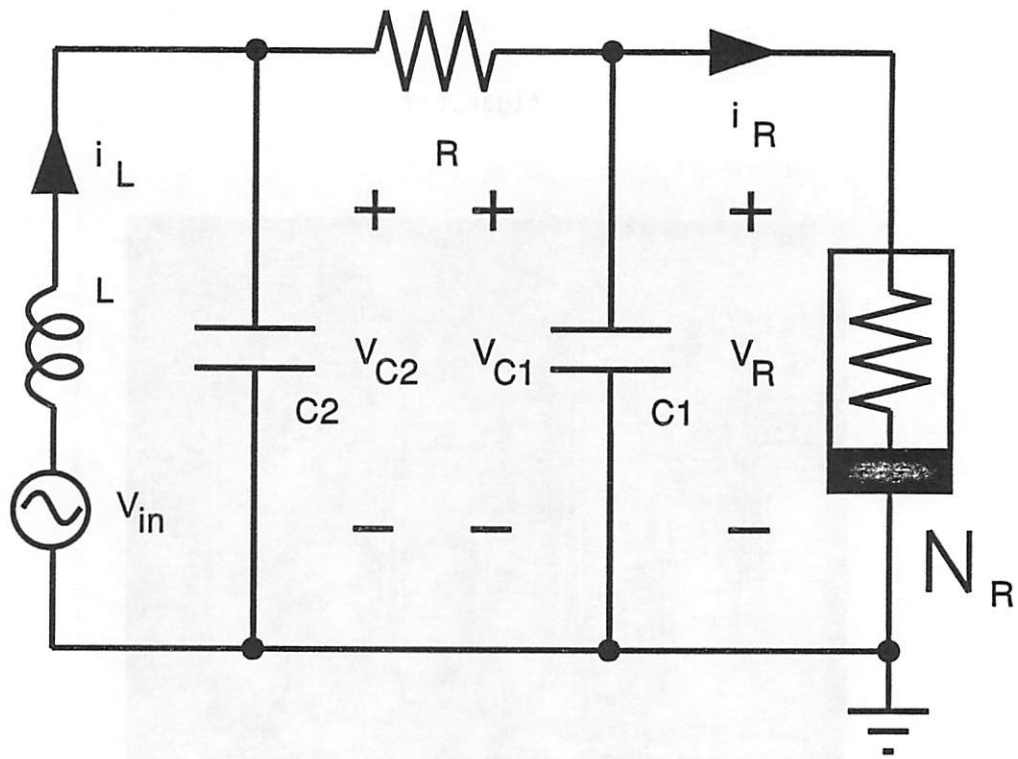


Figure 4a

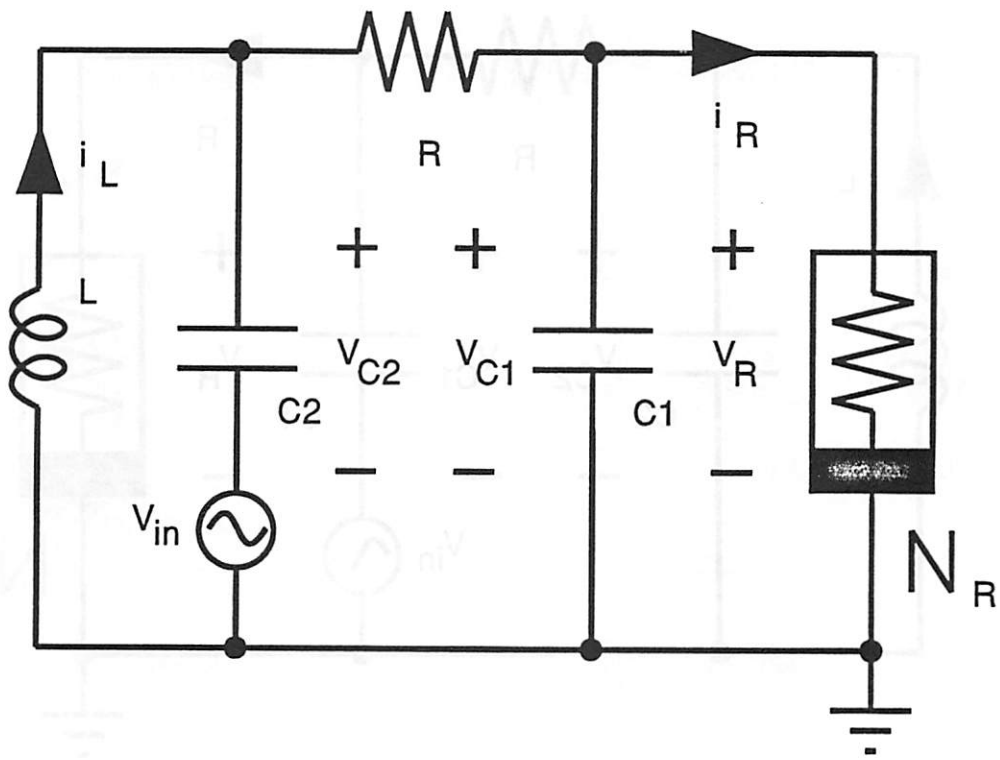


Figure 4b

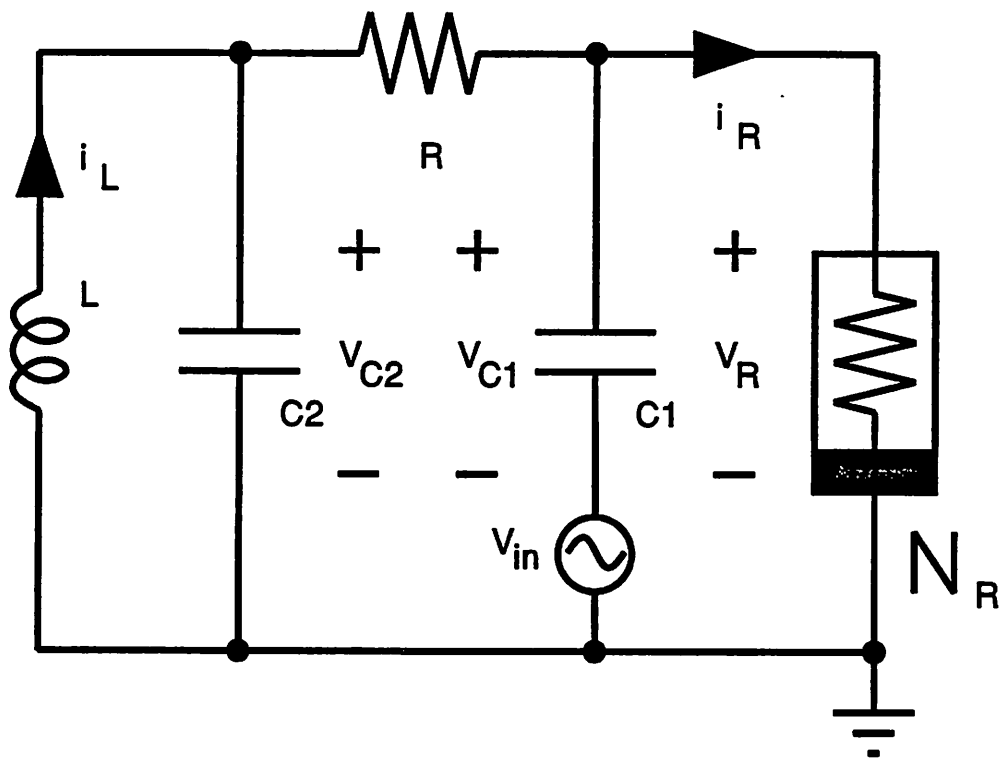


Figure 4c

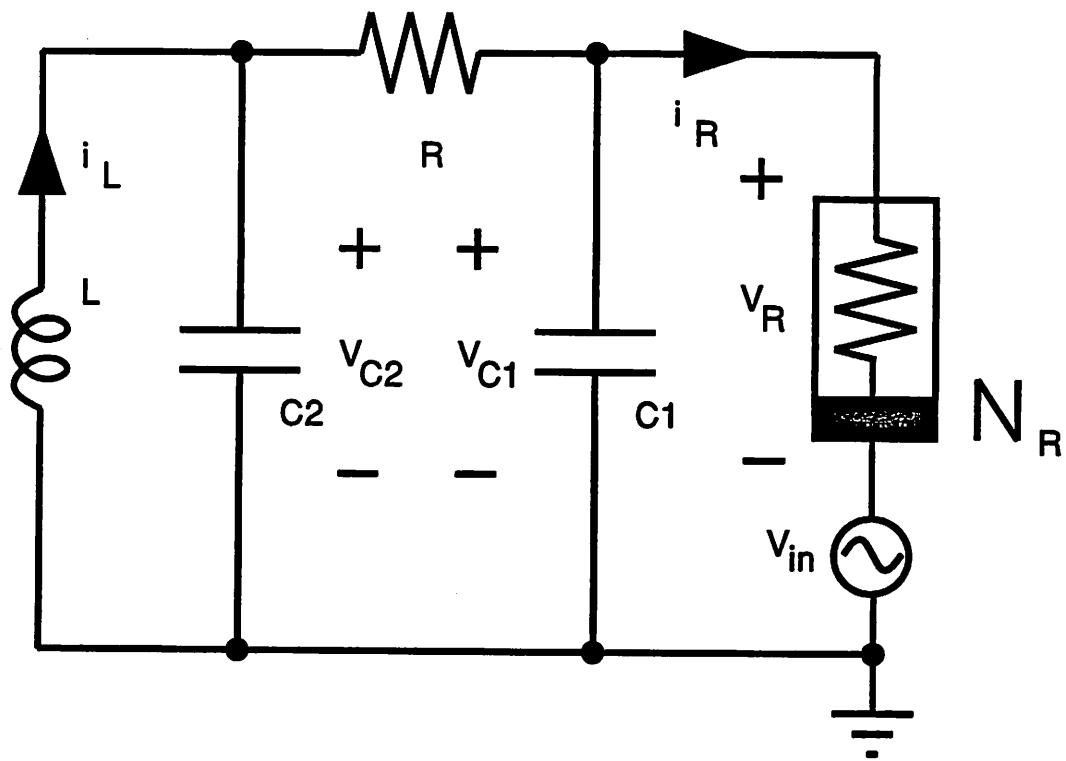


Figure 4d

~~fig5.tif~~

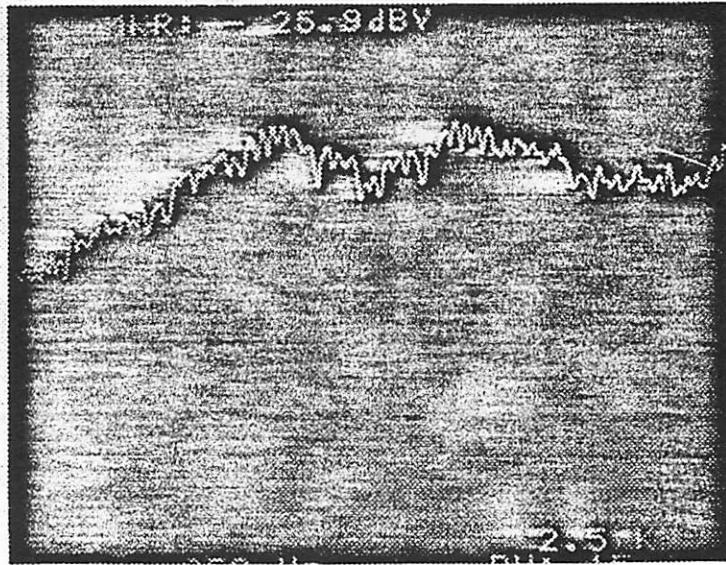


Figure 5a

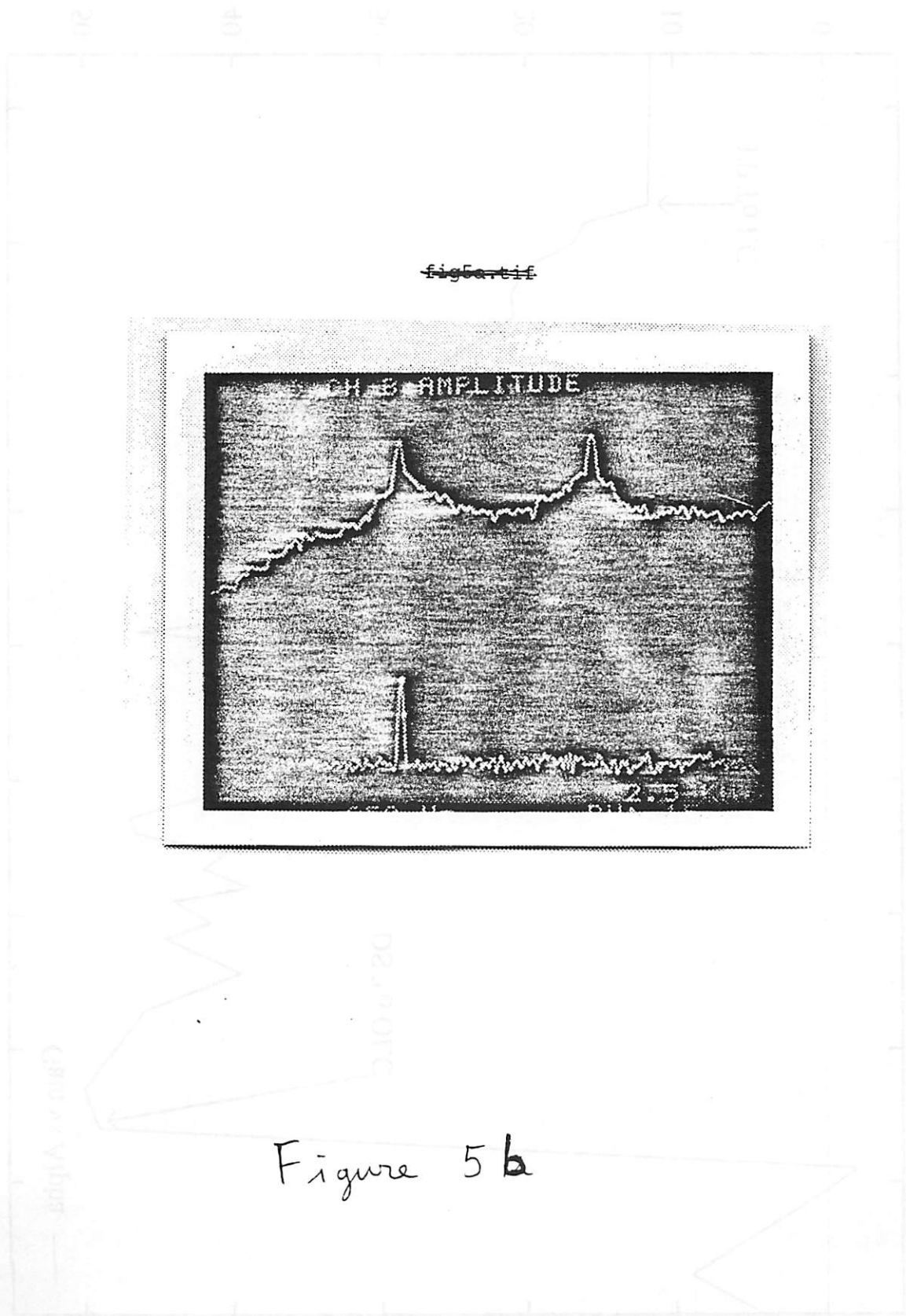


Figure 5b

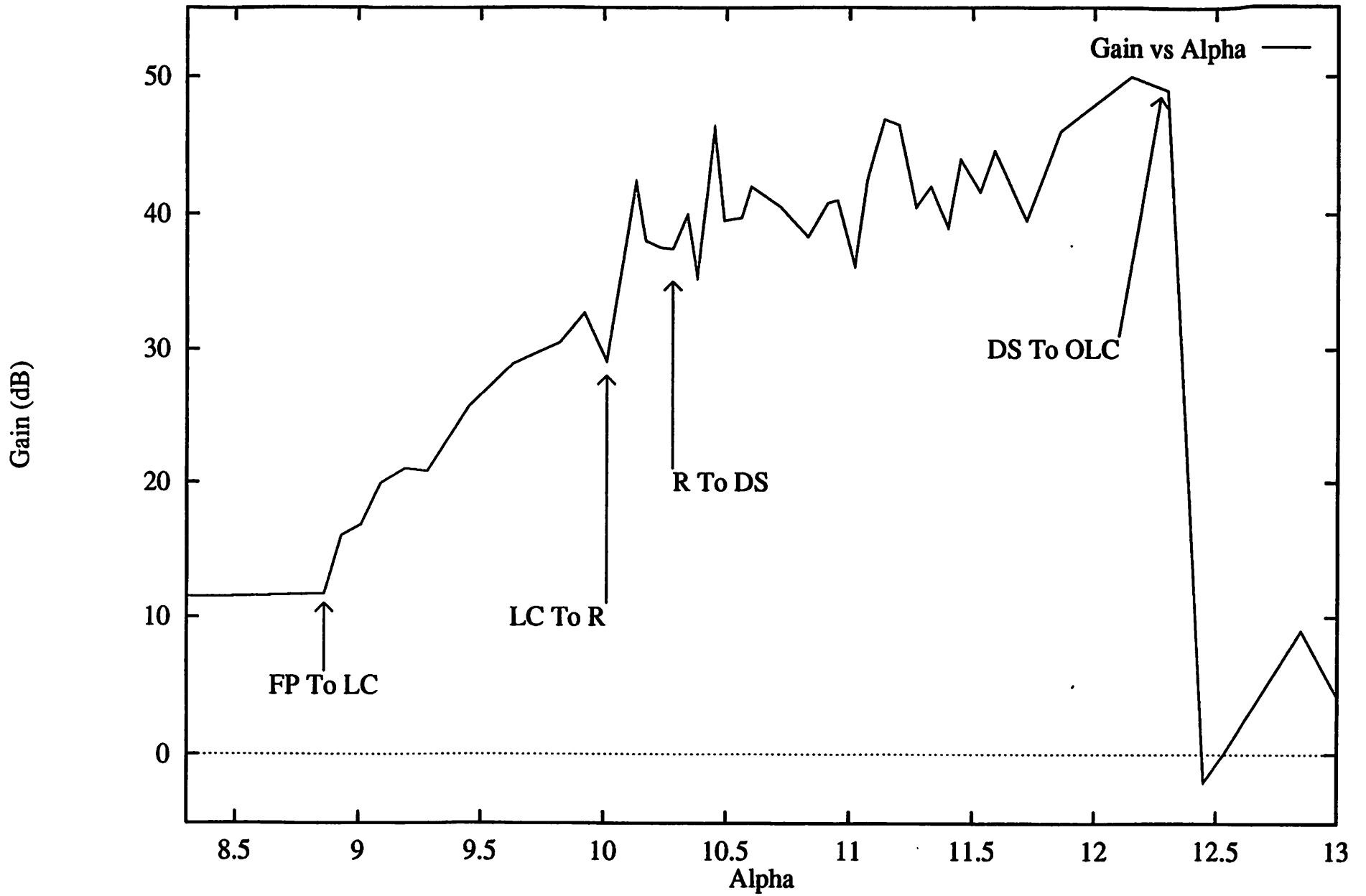


Figure 6

fig7.tif

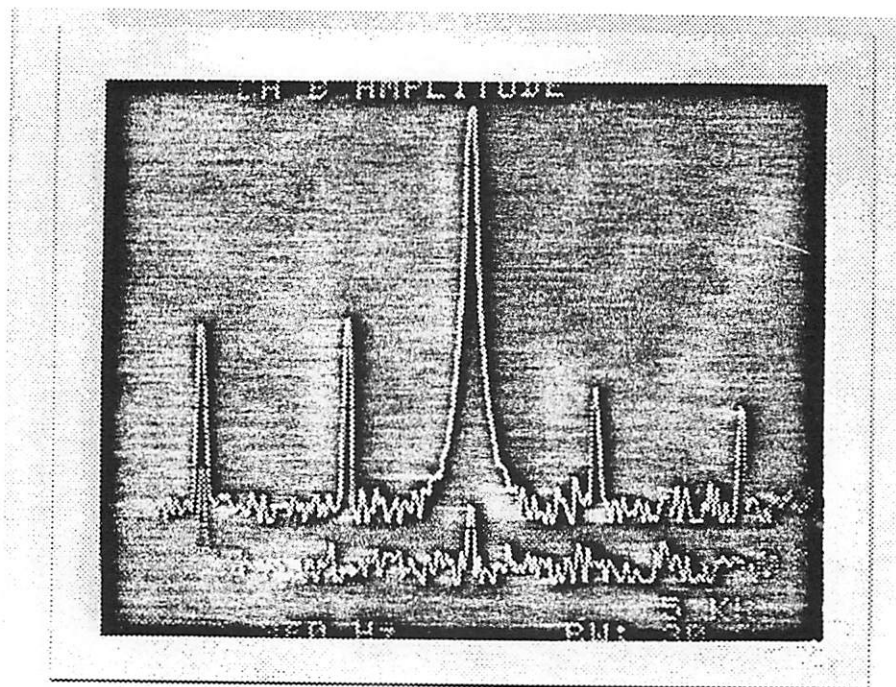


Figure 7

fig8.tif

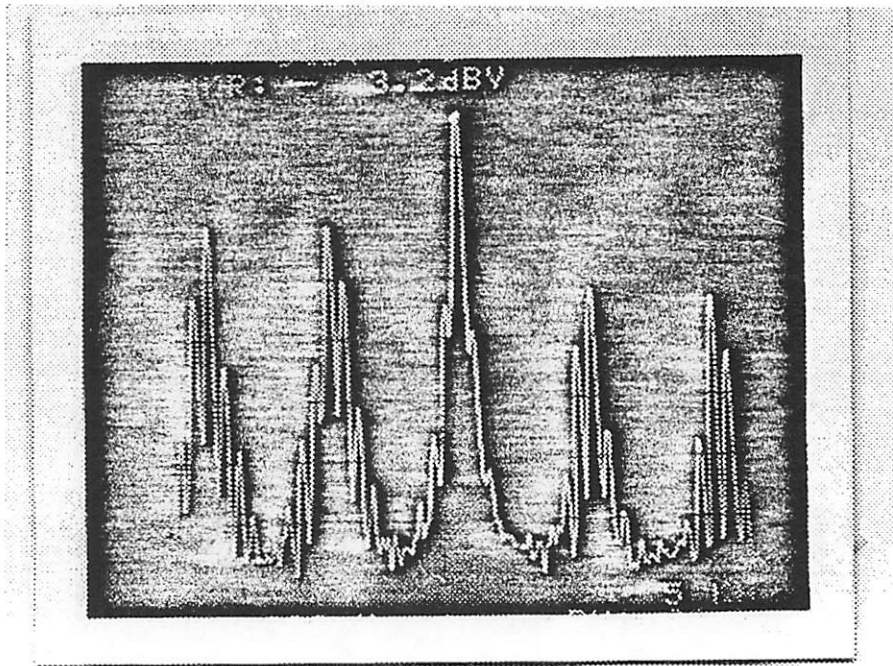


Figure 8

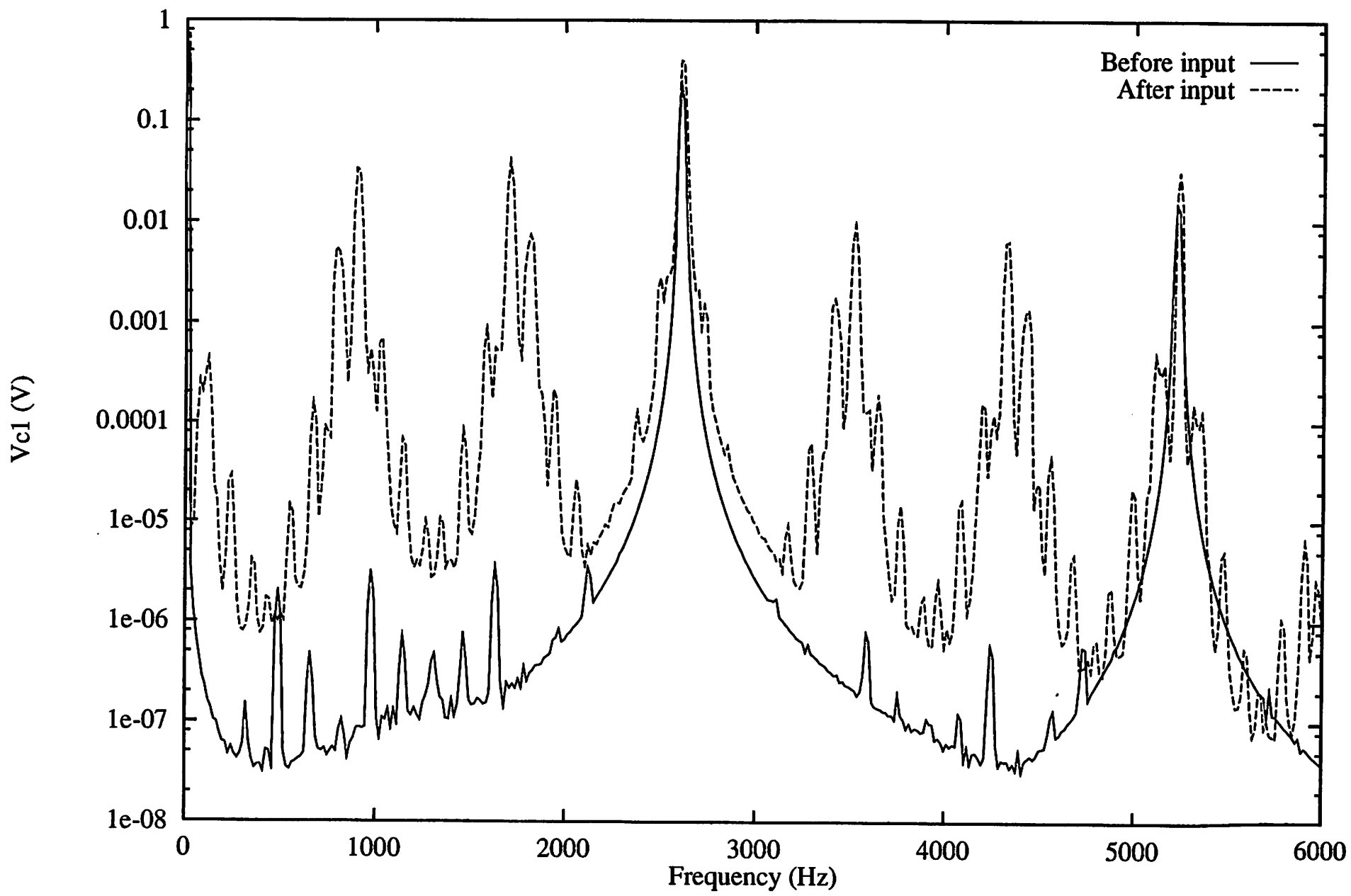


Figure 9

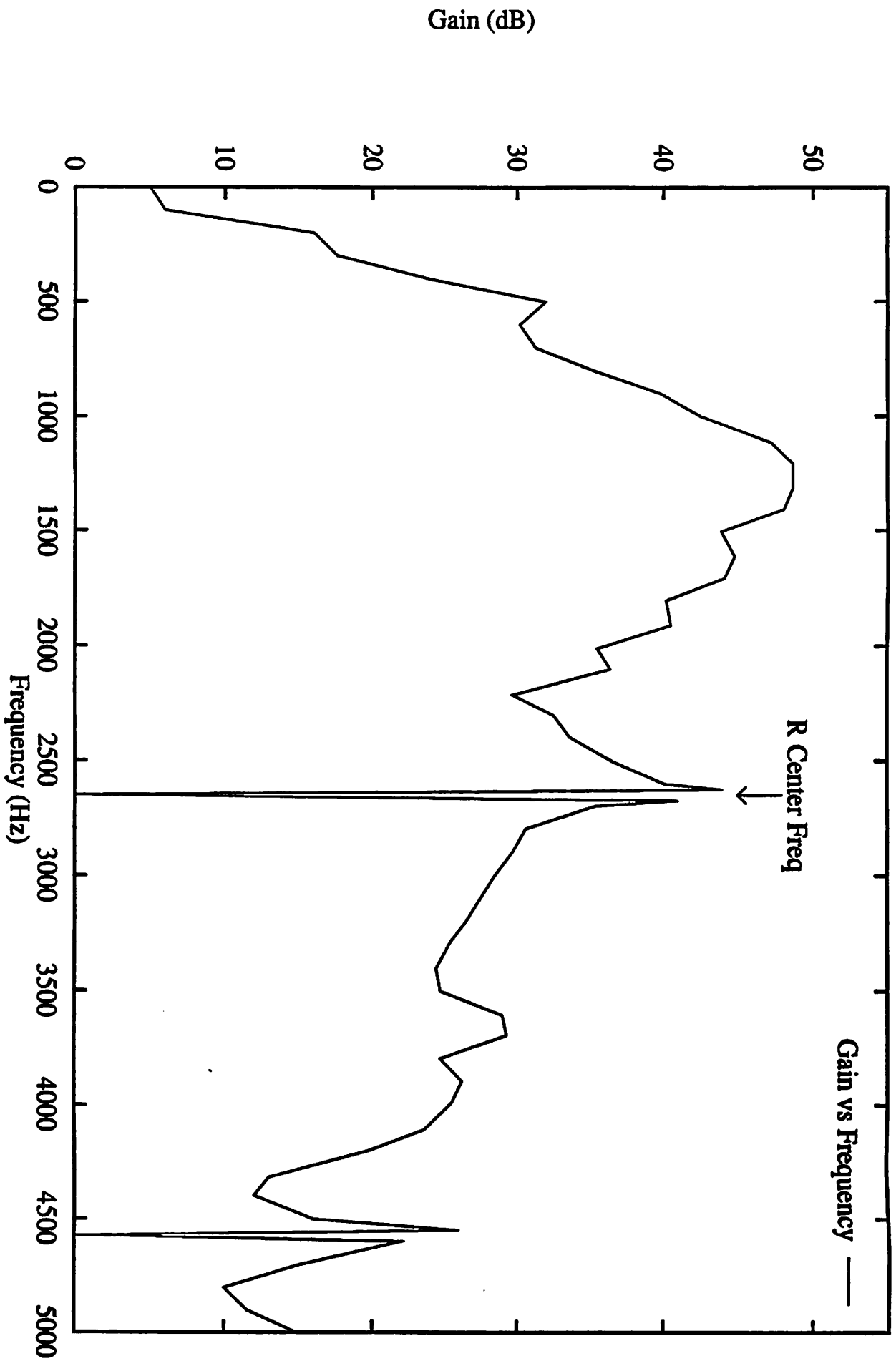


Figure 10

(8b) nioD

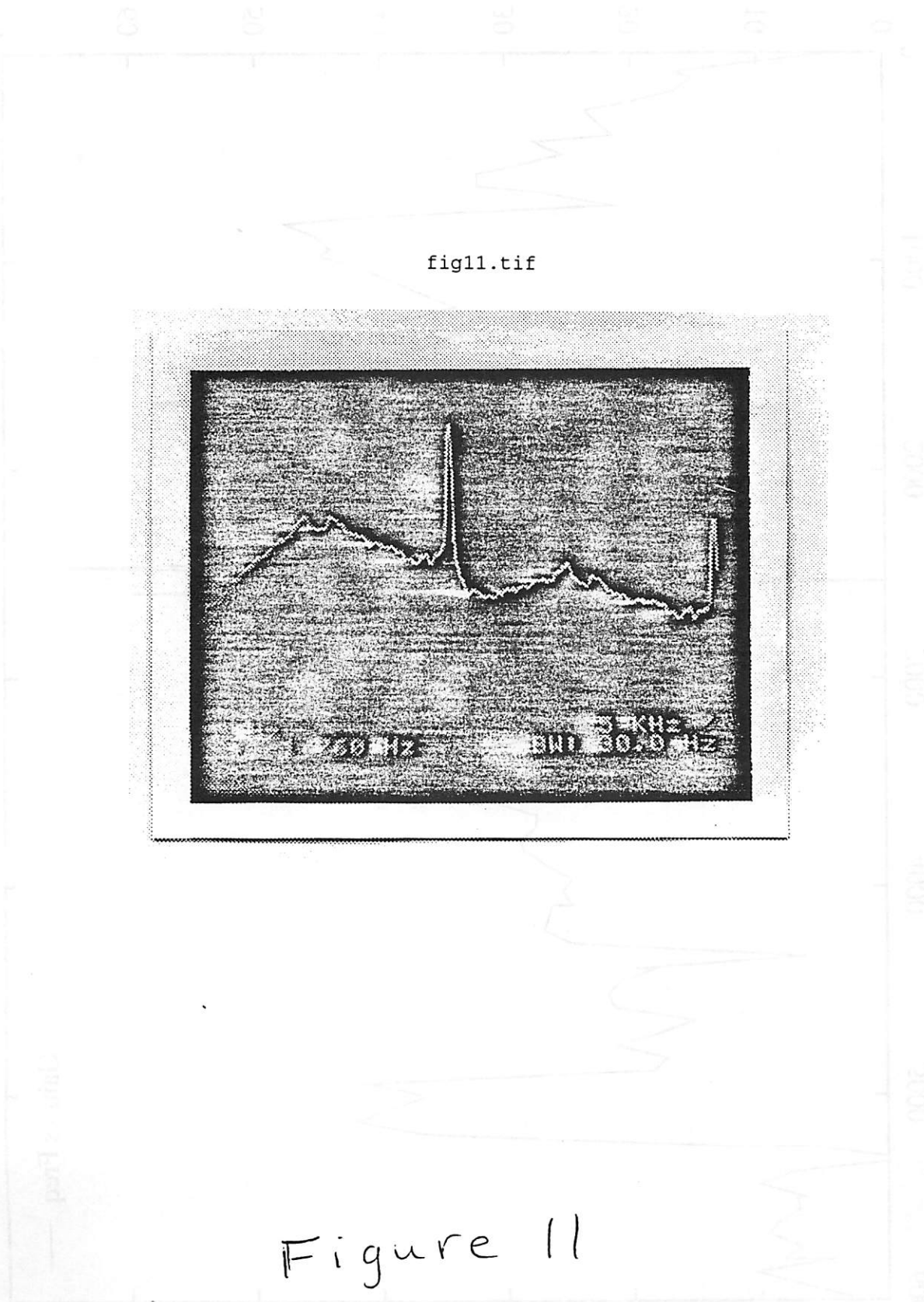


fig11.tif

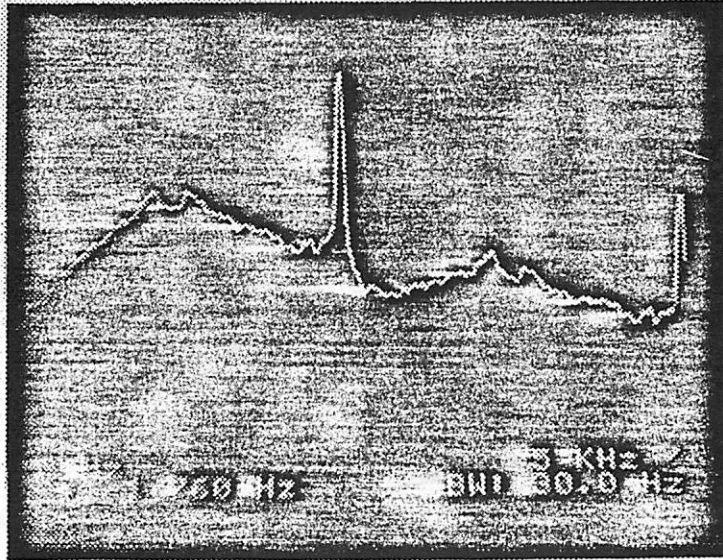


Figure 11

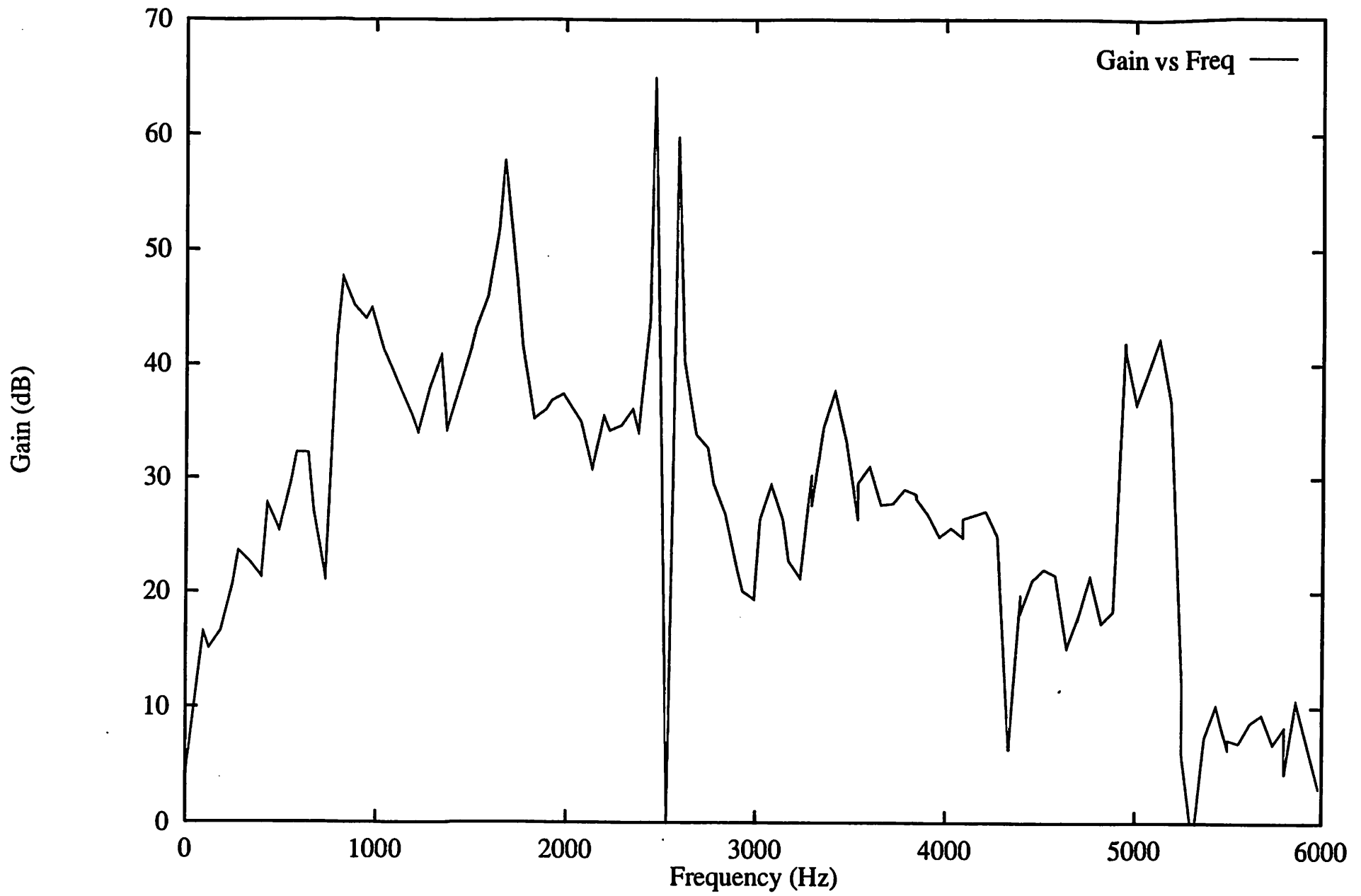


Figure 12

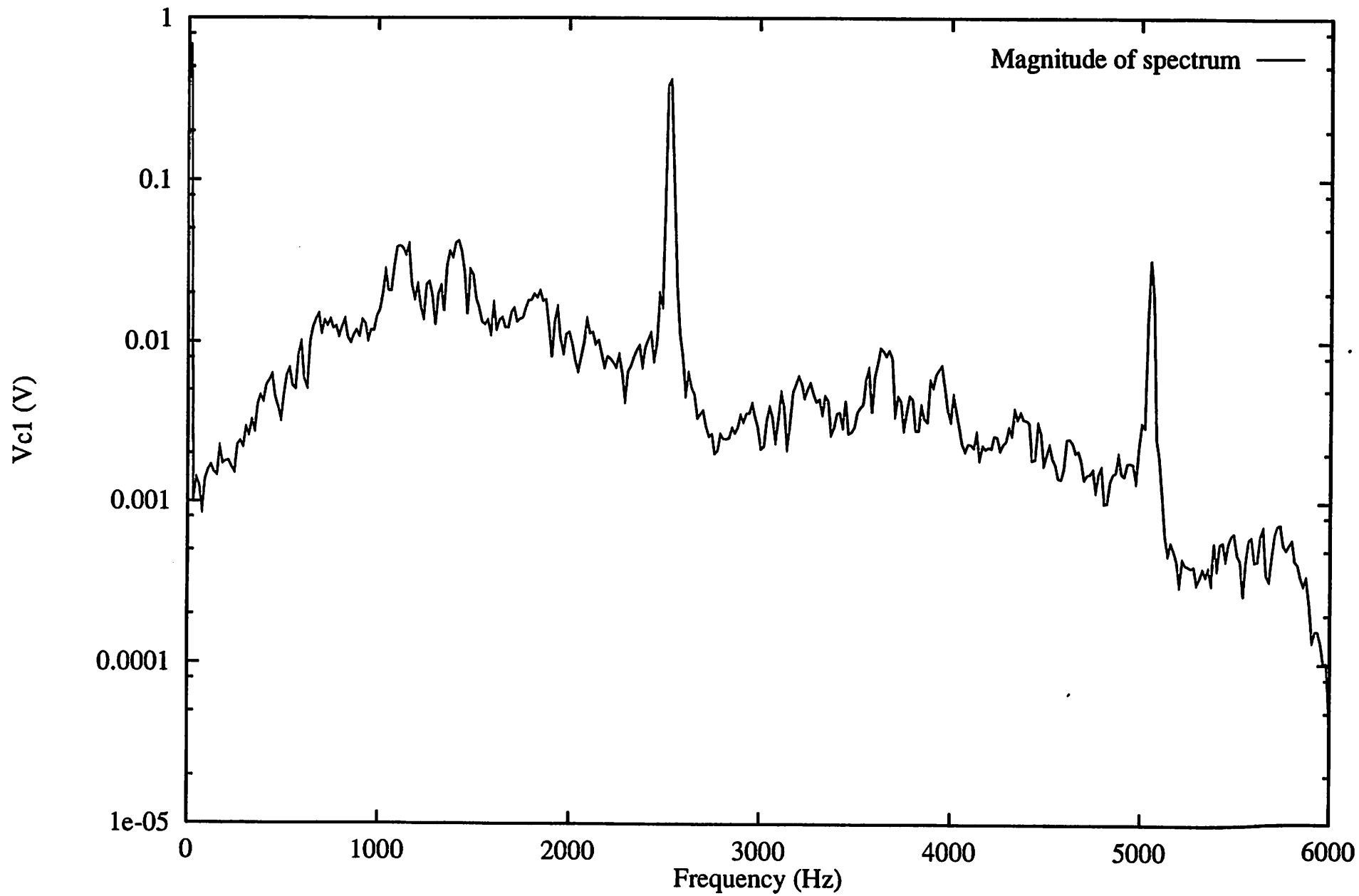


Figure 13

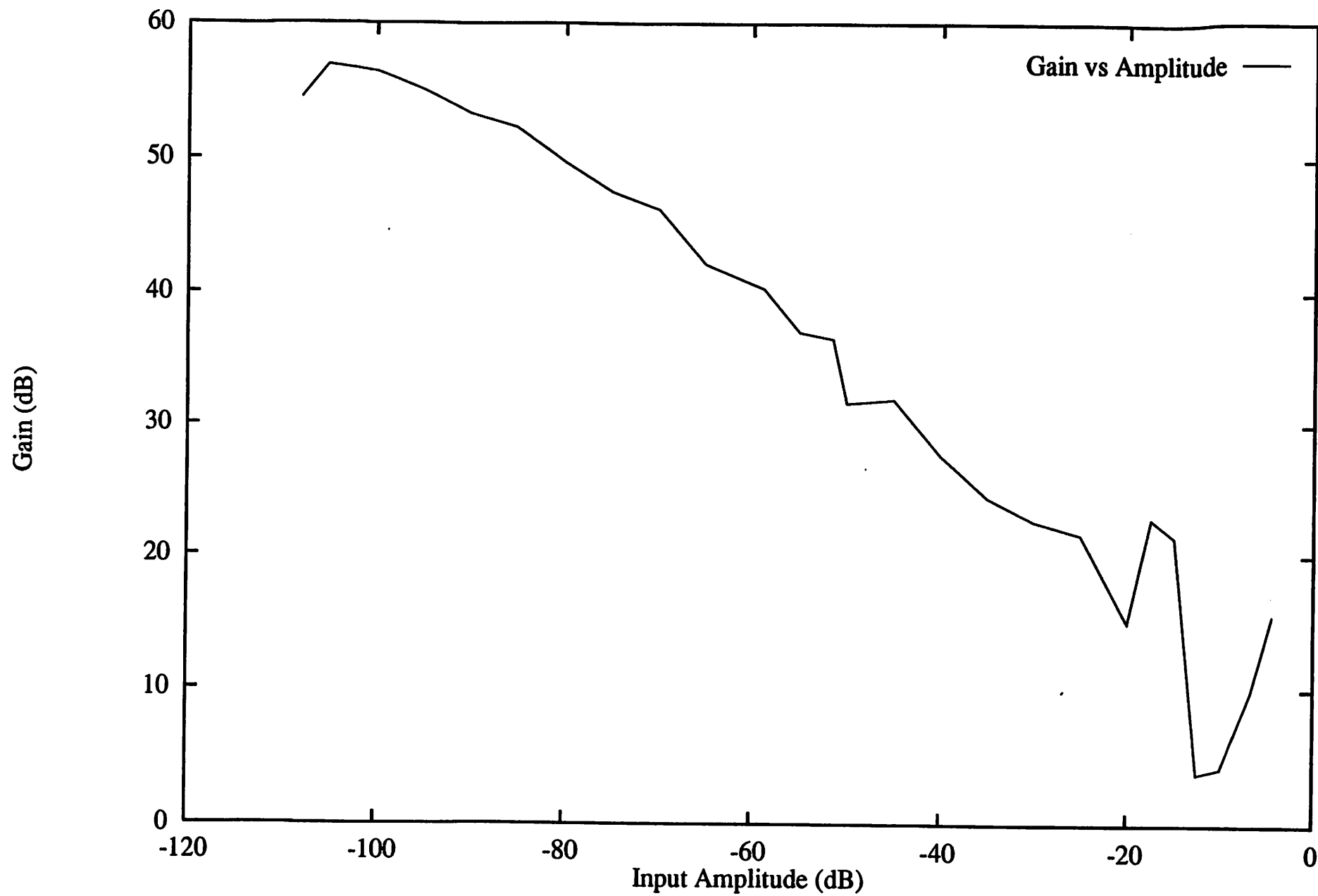


Figure 14

fig15.tif

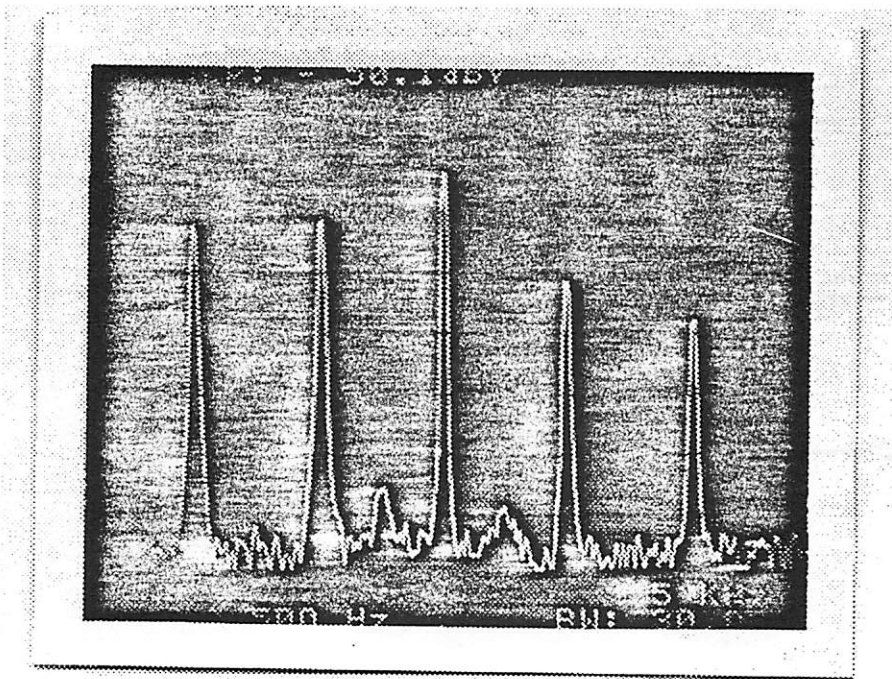


Figure 15

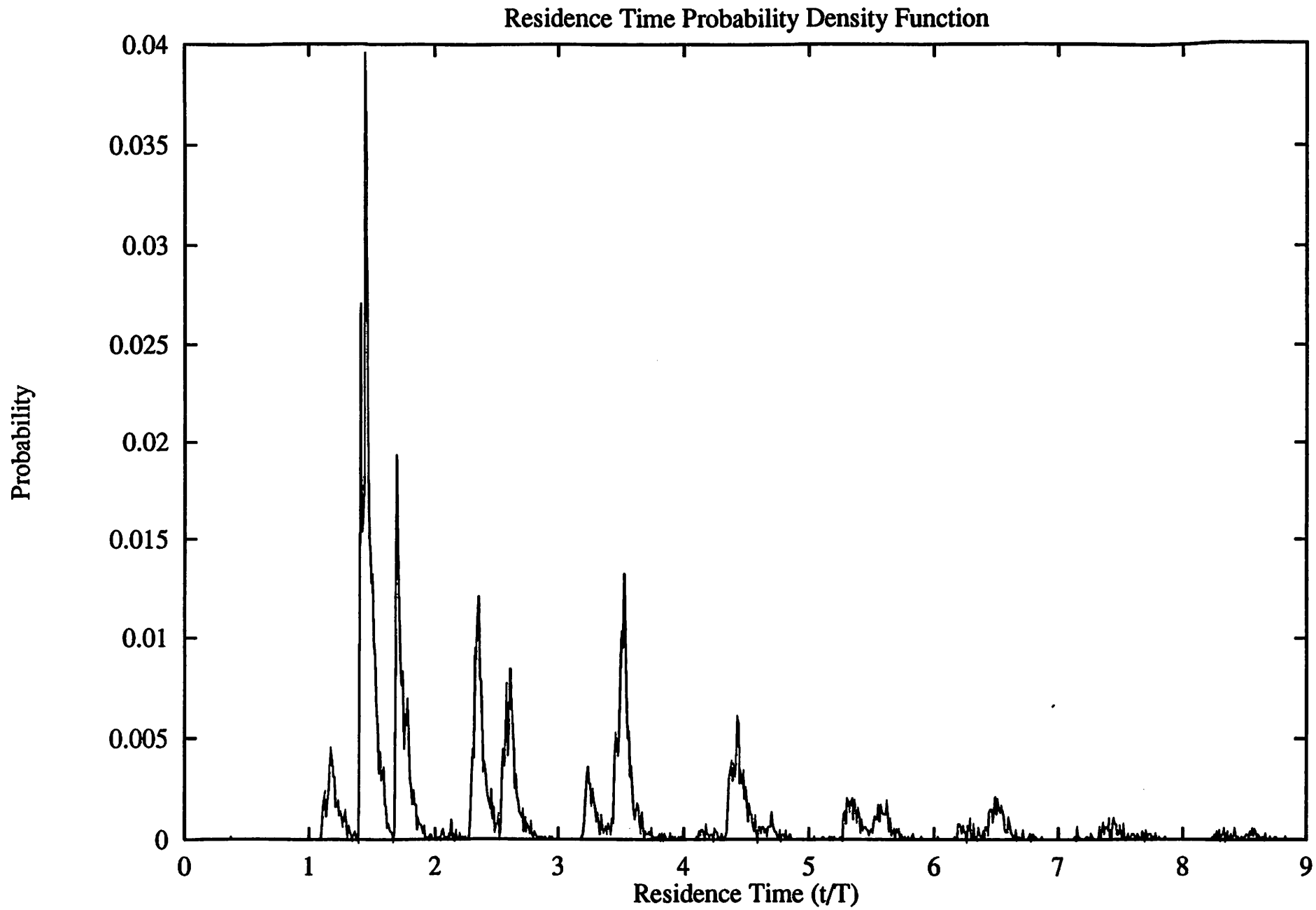


Figure 16

fig17cont.tif

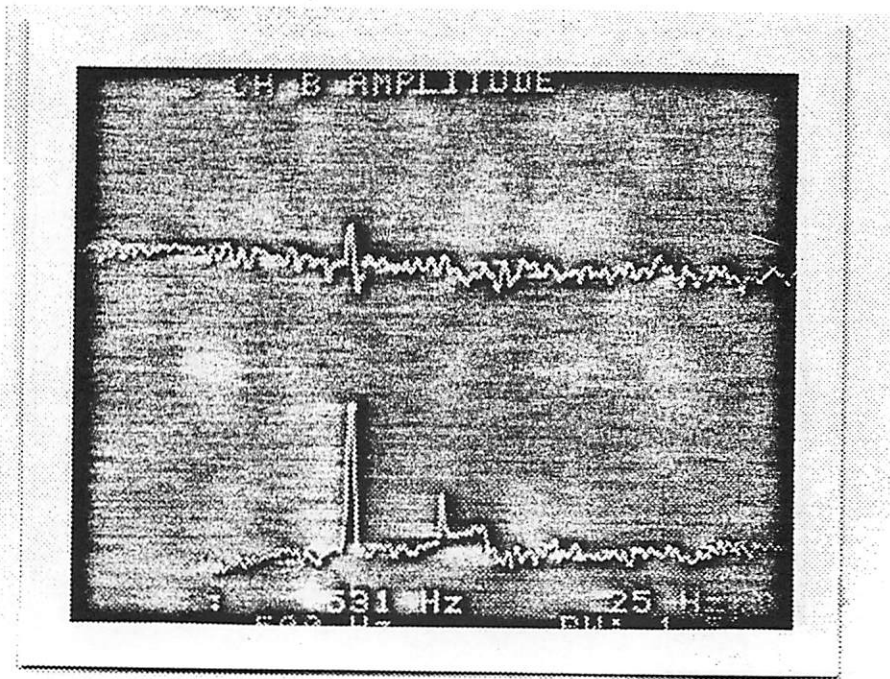


FIGURE 17a

~~Figure 17a~~

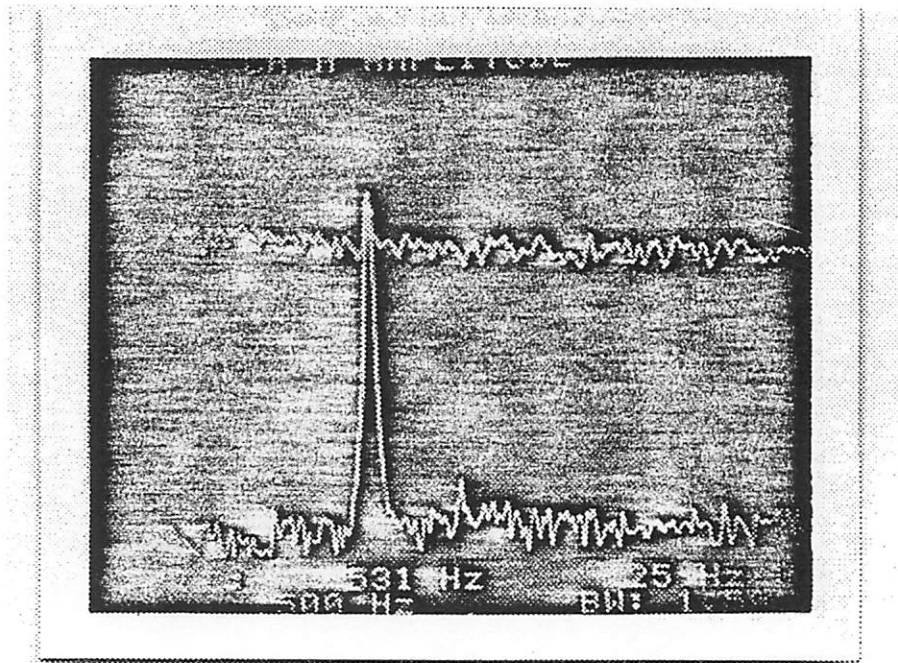


Figure 17b

~~fig17b.tif~~

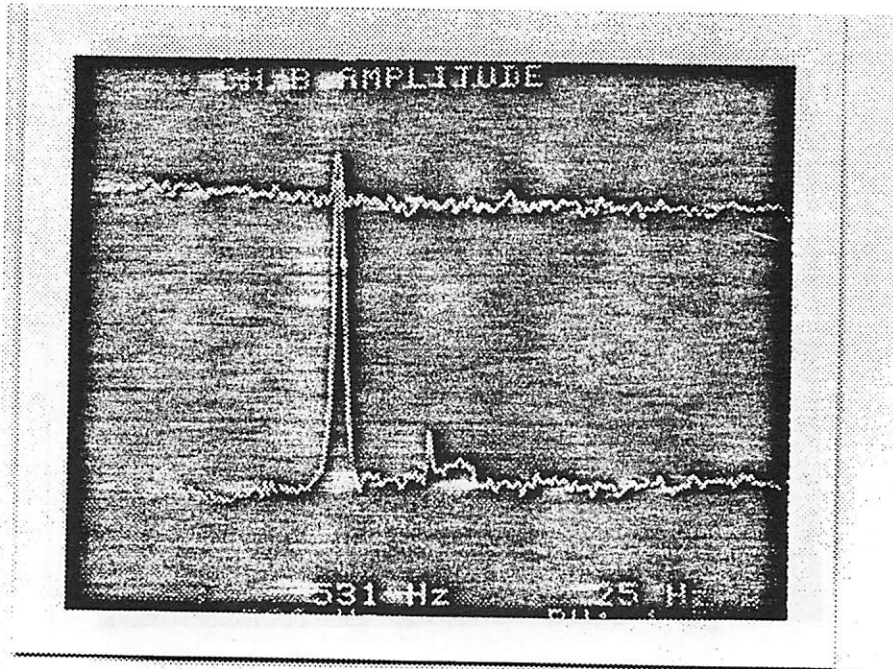


Figure 17c

~~fig17c.tif~~

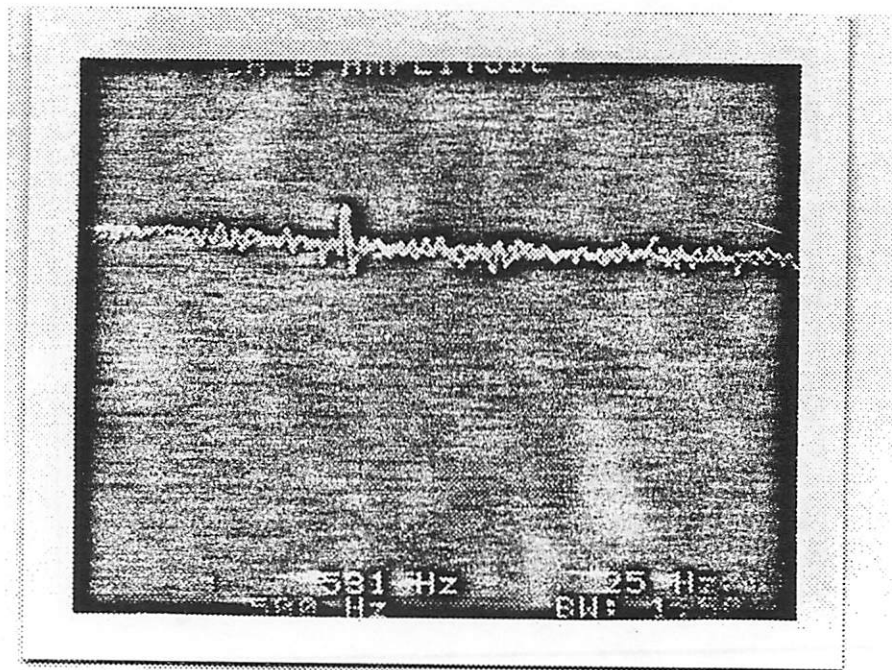


Figure 17 d

fig18.tif

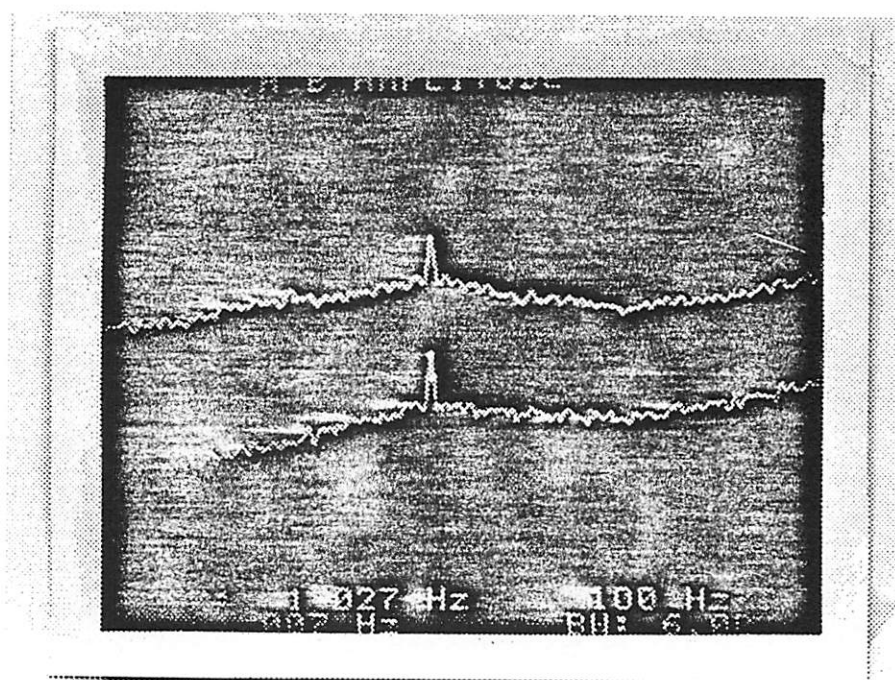


Figure 18